Proceedings of Japan- France Seminar on Chemical Evolution of Galaxies

STRUCTURE AND PHYSICS OF COOL GIANT MOLECULAR COMPLEXES

E. Falgarone and M. Pérault
Radioastronomie millimétrique, Ecole Normale Supérieure,
24 rue Lhomond, 75005 Paris, France

ABSTRACT. The interstellar medium is observed to be fragmented at all scales ranging from that of the supercloud complexes to that of the protostellar cores, forming a hierarchy which is not self-similar. In the solar neighbourhood, the self-similarity breaks down at a salient scale which we call that of 'clouds': their mass is several $100 M_\odot$, their size a few parsecs. The clouds, building blocks of the hierarchy, are supported against gravity by supersonic but subalfvénic turbulence. We show that this turbulence can be fed, via magnetohydrodynamic waves, over several 10^7 years, by a pumping of the orbital kinetic energy of the other clouds within the same complex. We also show that local gravitational instabilities may develop within the gravitationally stable clouds and eventually form dense protostellar cores.

We define *cool* GMC's as molecular complexes which have a mass, a size and an internal velocity dispersion typical of 'standard' GMC's ($M \sim$ a few $10^5 M_\odot$, maximal dimension $\sim 100\,\mathrm{pc}$, internal velocity dispersion $\sim$ a few km/s and therefore a mean density $\sim 10\,\mathrm{cm}^{-3}$) but unlike those GMC's are not associated with bright HII regions: they currently form stars as indicated by the large IR luminosity over mass ratio ($L/M \sim 10$) of a few active fragments but no ionizing stars ($M_* > 15\,M_\odot$).

1. Large and small scale millimeter lines observations: spatial and velocity structure of cool GMC's

The observations referred to here are extensively described and discussed in Pérault et al. 1985 (PFP). The complexes (or part of complexes) which we mapped in the ^{13}CO(J=1-0) line were selected on the basis of their low far infrared brightness in balloon borne surveys of the Galaxy (Gispert et al. 1982): they appear to be also characterized by a low ^{12}CO brightness temperature compared to that of the Cygnus complex for example. We show on Fig. 1 (from Dame and Thaddeus 1985) the areas that we have mapped together with, in each case, the adopted distance to the complex.

Large scale mapping was achieved with the Bordeaux telescope ($HPBW \sim 4.4'$) in the ^{13}CO(J=1-0) line. Smaller scale observations carried out with various telescopes at different wavelengths provided us with additional increasing angular resolutions

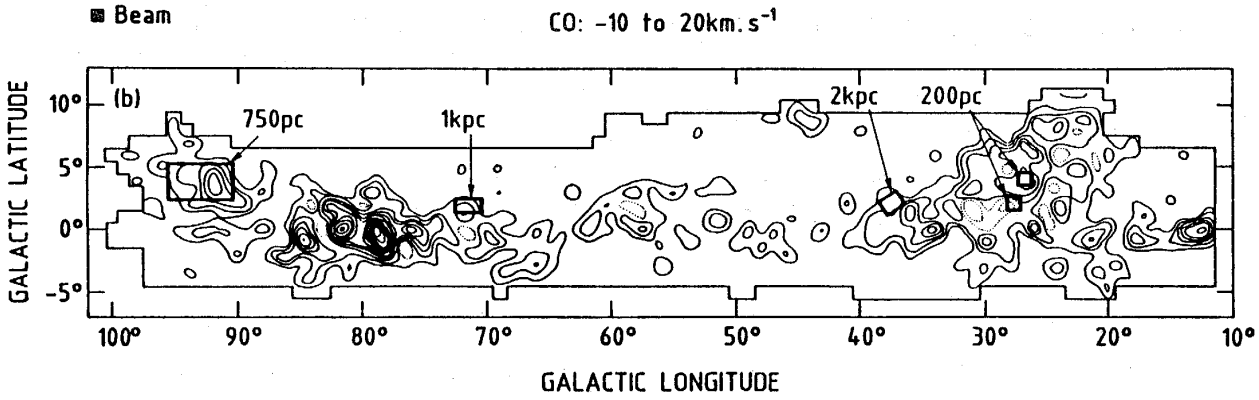

Fig. 1. ^{12}CO contours of the Galactic plane from Dame and Thaddeus (1985) on which are drawn the areas which have been mapped in the ^{13}CO line with the Bordeaux antenna. The estimated distance is indicated above each complex.

of 1.4′ with the MWO antenna, 49″ with the FCRAO antenna and 20″ with the IRAM-30m telescope. The distances to the selected complexes range between 150 pc and 3.2 kpc: thus the range of linear scales resolved by our observations and of the sample sizes span more than one order of magnitude (respectively 0.18 pc to 4.2 pc and 3 pc to 60 pc).

One of the most conspicuous results of these observations is the prominence of the highly fragmented and dispersed structure (in space as well as in velocity) of these complexes: their molecular mass, as traced by the ^{13}CO emission, is *not* distributed throughout the complexes volume but is concentrated in *clouds*, the masses of which cover a large range: $10\,M_\odot$ to $5 \cdot 10^4\,M_\odot$. We focus here on two specific points relying on a few examples drawn from this set of observations.

1.1. The ambiguity of a cloud mass spectrum in a hierarchical structure

Let's start with the misleading concept of mass spectrum: our observations as well as those of others on brighter GMC's, reveal unambiguously that most of the clouds in molecular complexes belong to a clear hierarchical structure (see below) in which apparently all the scales are populated. In addition, this hierarchy is *not self-similar*: the fraction of the mass of a given scale which lies in the clouds of the subsequent scale and not in the intercloud medium clearly decreases toward small scales.

We consider first the most remote complex, located around $l = 37.6°$, $b = 2.3°$ with an estimated distance of 3.2 kpc (see PFP). The ^{13}CO emission is split into several velocity components (Figs. 2a and 2b). The most intense emission comes from a ~ 30 pc cloud centered at $v = 32$ km/s which itself breaks up into 7 spatially unresolved clouds (size < 2.6 pc) but resolved in velocity. The (l, b, v) positions of these subclouds may be found on the velocity maps of Fig. 2c. Quantitative estimates of their parameters will be given in Section 1.2: the main result is that half of the total integrated emission of the $v = 32$ km/s cloud arises in these 7 subclouds. Since no smaller scale observations are yet available for this complex, we can not assess where the rest of the emis-

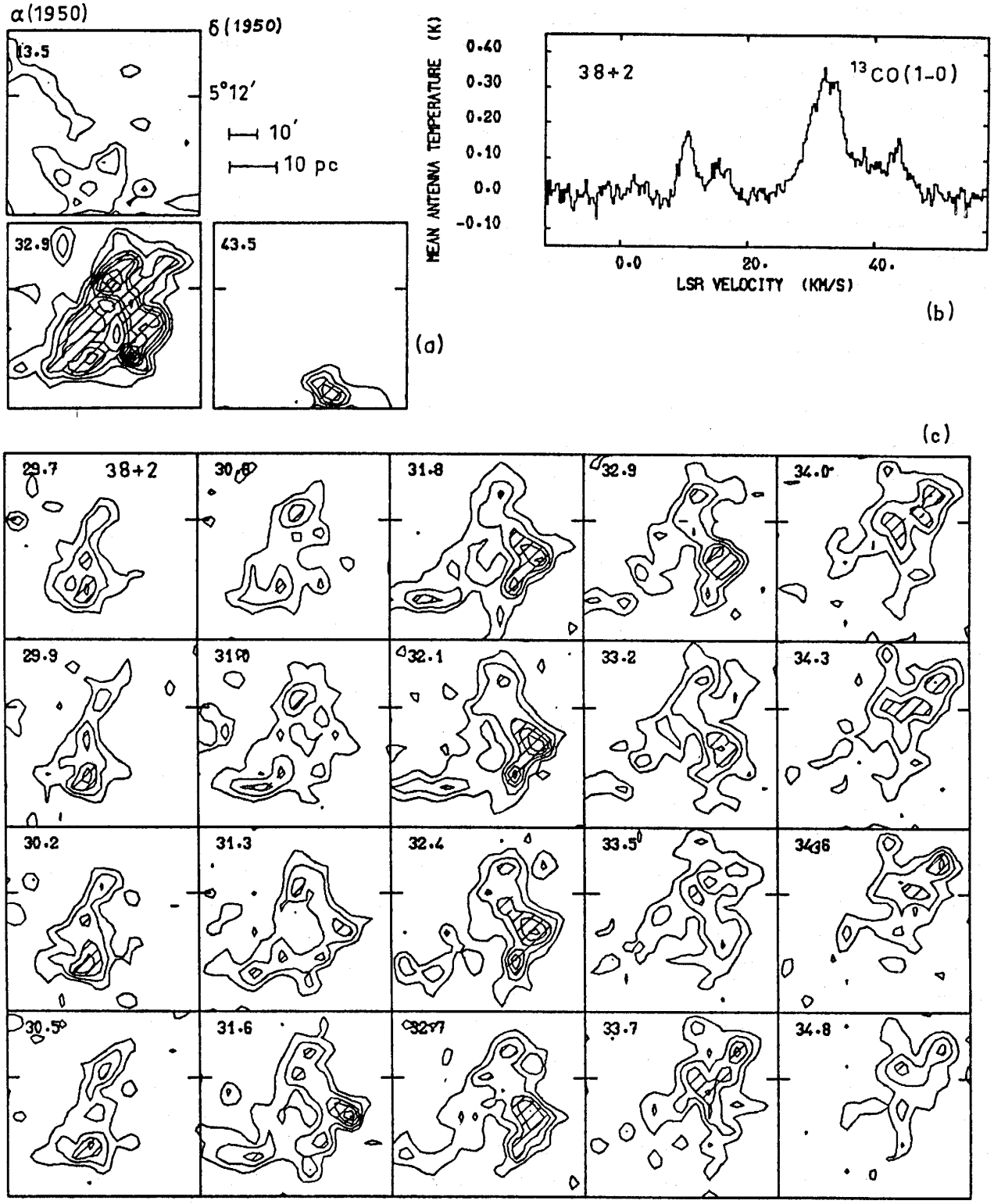

Fig. 2. The G37+2 field (reference position $\alpha(1950) = 18h49m12s$, $\delta(1950) = 5°12'$) in the $^{13}CO(J=1-0)$ line with 4.4′ resolution. (a) Maps of integrated emission in three broad channels centered on the velocities indicated in the upper left corners. The contour interval is 1 K km/s. (b) Velocity profile averaged over the field (1.6 square degree or $1.9 \cdot 10^3$ pc^2). (c) Channel maps over a large fraction of the main velocity component; contour interval 0.4 K.

sion comes from: is it distributed within the parent cloud volume or does it come from a large number of unresolved clouds with a surface filling factor > 1 and a volume filling factor in the parent cloud much smaller than 1? A crude estimate of the gas mean density in the former case (assuming a spherical geometry) is $\bar{n} = 90\,\mathrm{cm}^{-3}(R/10\,pc)^{-1}$: this value is too close to the local density required to collisionally excite the ^{13}CO line to allow any definite conclusion.

One therefore may ask: should this object be accounted for, in a mass spectrum, as one massive object of mass M, as seven clouds of mass $M/14$ plus one of mass $M/2$ (the distributed intercloud medium) or as seven clouds of mass $M/14$ plus a number N of low mass ($M/2N$) clouds (once they have been resolved)?

1.2. The hierarchy is not self-similar down to 0.1 pc

The second complex lies close to the Cygnus complex around $l = 94°$, $b = 3°$ (Fig. 1). It extends over $\sim$ 100 pc at the estimated distance of 750 pc (see PFP). On the map of the integrated ^{13}CO emission displayed in Fig. 3a, the first level corresponds to $A_v \sim 1$ mag (according to the simple relation valid in this range of column density: $A_v \sim \int T_A^*(^{13}\mathrm{CO})dv$ (in K km/s)). The surface filling factor of the gas detected above this level is close to 1. When displayed in different velocity ranges the emission is far from keeping $f_s \sim 1$ (Fig. 3b). It breaks up into smaller entities (down to the resolution of the observations) which are either isolated or gathered into larger structures of various mass.

Smaller scale observations have been carried out with several telescopes in the three areas (C1 to C3) delineated in Fig. 3a. Contrary to what happens at the 100 pc scale, clouds like C1, C2 or C3 which appear on channel maps as isolated clouds (hardly resolved in the case of C2 with the larger beam) *do not* break up into several subclouds when observed at higher angular resolution in the same isotope of CO (see Fig. 9 of PFP).

Another example is given in the maps of Fig. 4: they show contours of ^{13}CO intensity integrated over consecutive channels in a region of the Taurus-Perseus complex which can be identified on the large scale CO map of Ungerechts and Thaddeus (1986). Clouds with similar characteristics as in the previous complex can be identified on these maps: again, they are clearly resolved and do not break up into smaller entities when observed with a beam much smaller than their size. The typical size of clouds T1, T2, T3 (although not entirely mapped) is about 4 pc at the estimated distance ($\sim$ 400 pc) of that part of the Taurus complex (Ungerer et al. 1985). This is our second point: at that scale in the hierarchy, the ^{13}CO emission is distributed throughout the *cloud* volumes, unlike what occurs at larger scales and we infer that a scale exists, in the hierarchy, within which the molecular mass is no longer distributed into smaller and much denser substructures but fills the whole volume.

Substructures, however, are clearly seen at small scale within these clouds in the C^{18}O(J=1-0 and J=2-1) lines (see Fig. 8 of PFP and Falgarone et al. 1984) down to

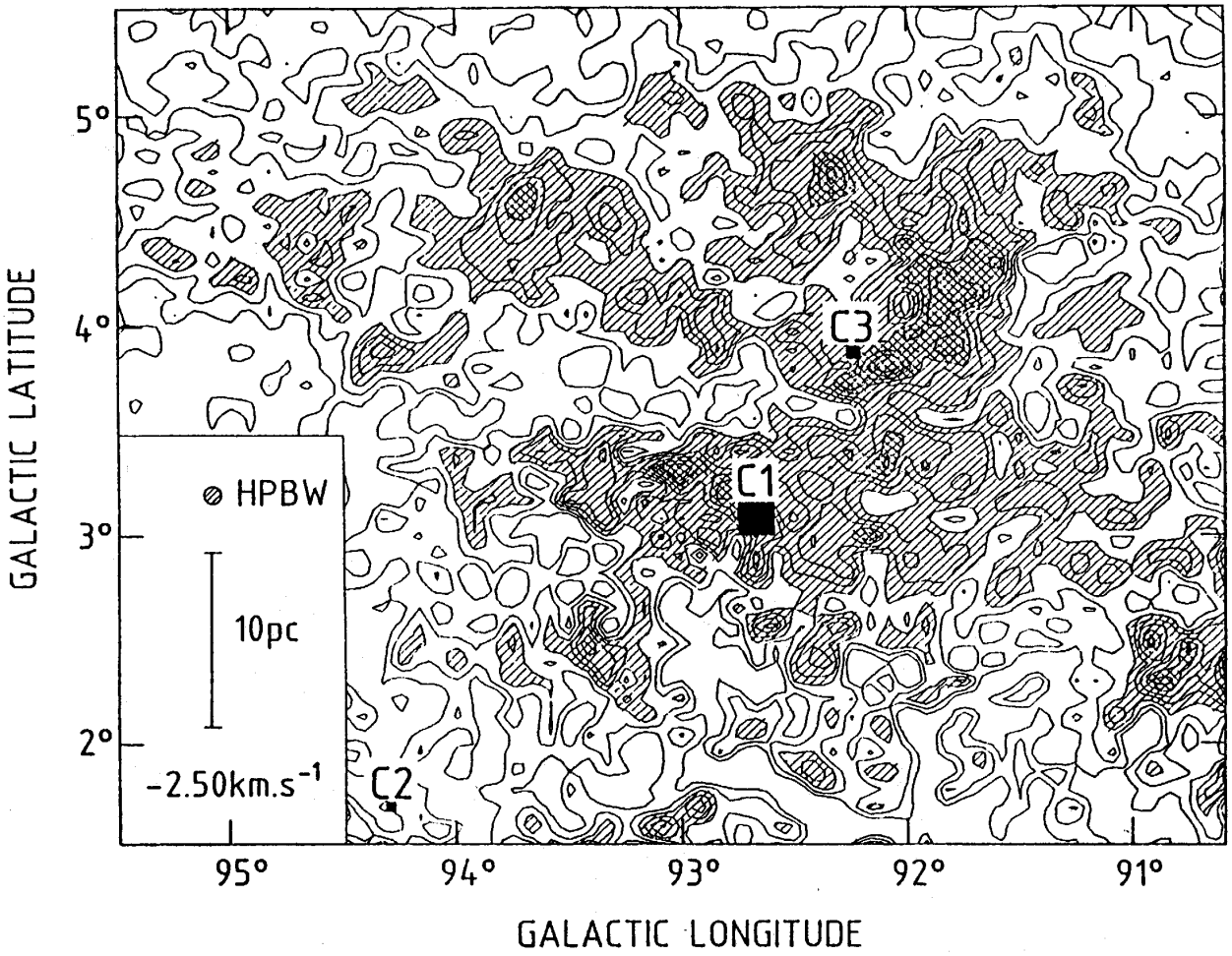

Fig. 3a. The G94+3 field in the ^{13}CO(J=1-0) line. Map of the integrated emission. The contour interval is 1 K km/s. Areas called C1, C2 and C3 which have been mapped at higher angular resolution are indicated.

0.07 pc and 0.14 km/s (IRAM-30m and MWO observations, Pérault and Falgarone 1987). But the mass contained in these *cores* is less than 10% of the cloud mass.

1.3 The cloud mass and internal velocity dispersion versus size relations

We measured the molecular mass, radius and internal velocity dispersion of 68 clouds belonging to 9 different complexes. In each complex, the clouds were defined as resolved connex volumes in the (l, b, v) or (α, δ, v) space in which the integrated ^{13}CO emission raises above a threshold close to 1 K km/s. We also selected those objects for which the brightness distribution $T_A^*(^{13}\mathrm{CO})(l, b, v)$ could be reasonably well fitted by a Gaussian in space and velocity. Details on the procedure, especially for the case of overlapping volumes, are given in Pérault (1987). From the Gaussian fits to the brightness distribution of each cloud along the velocity axis on the one hand and along the two space axis, on the other hand, we derive the dispersions σ_x, σ_y and σ_v from which, after de-

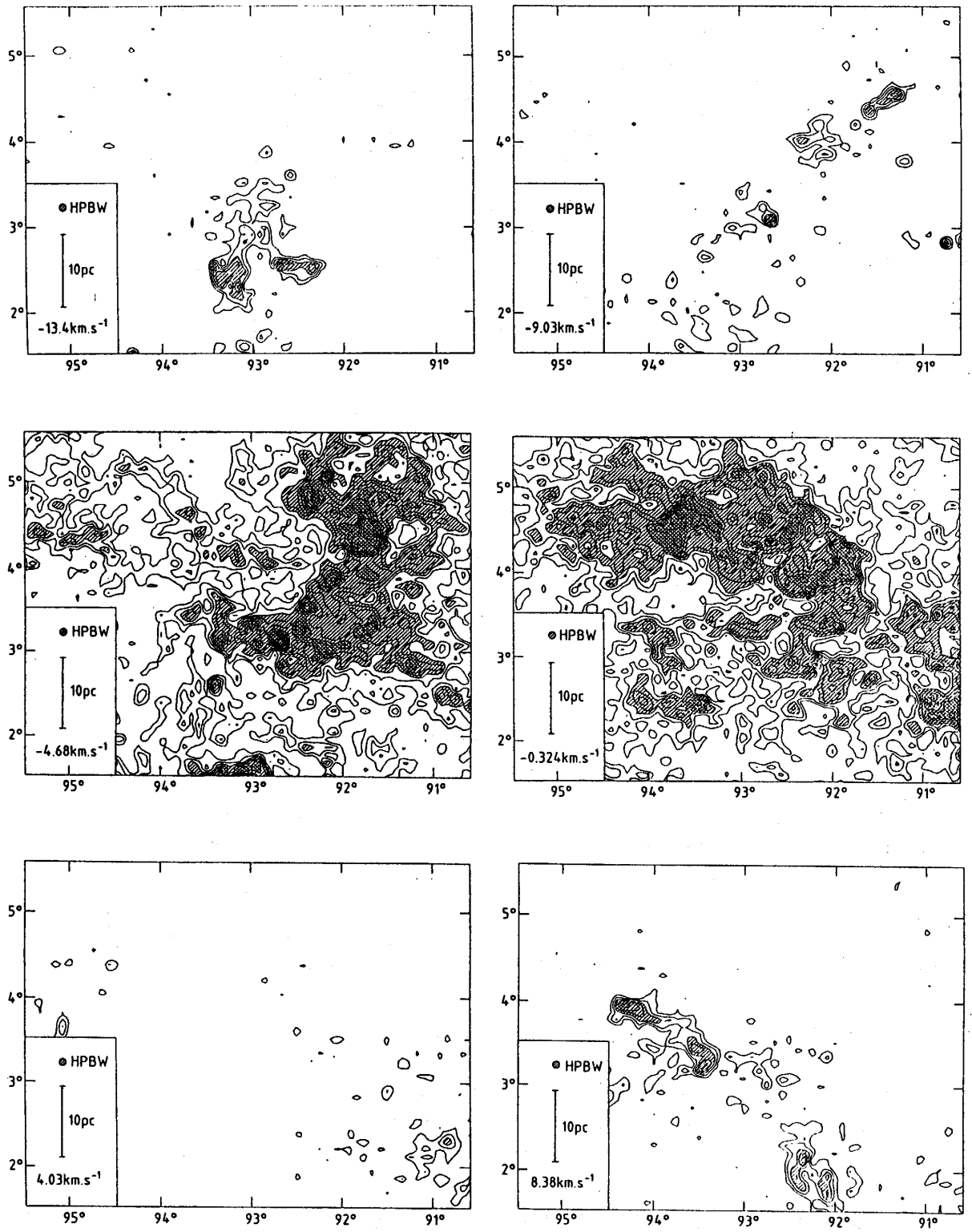

Fig. 3b. The G94+3 field in the $^{13}CO(J=1-0)$ line. Maps of the emission integrated over a few selected broad channels ($\delta v = 4.35\,km/s$). The contour interval is 0.5 km/s.

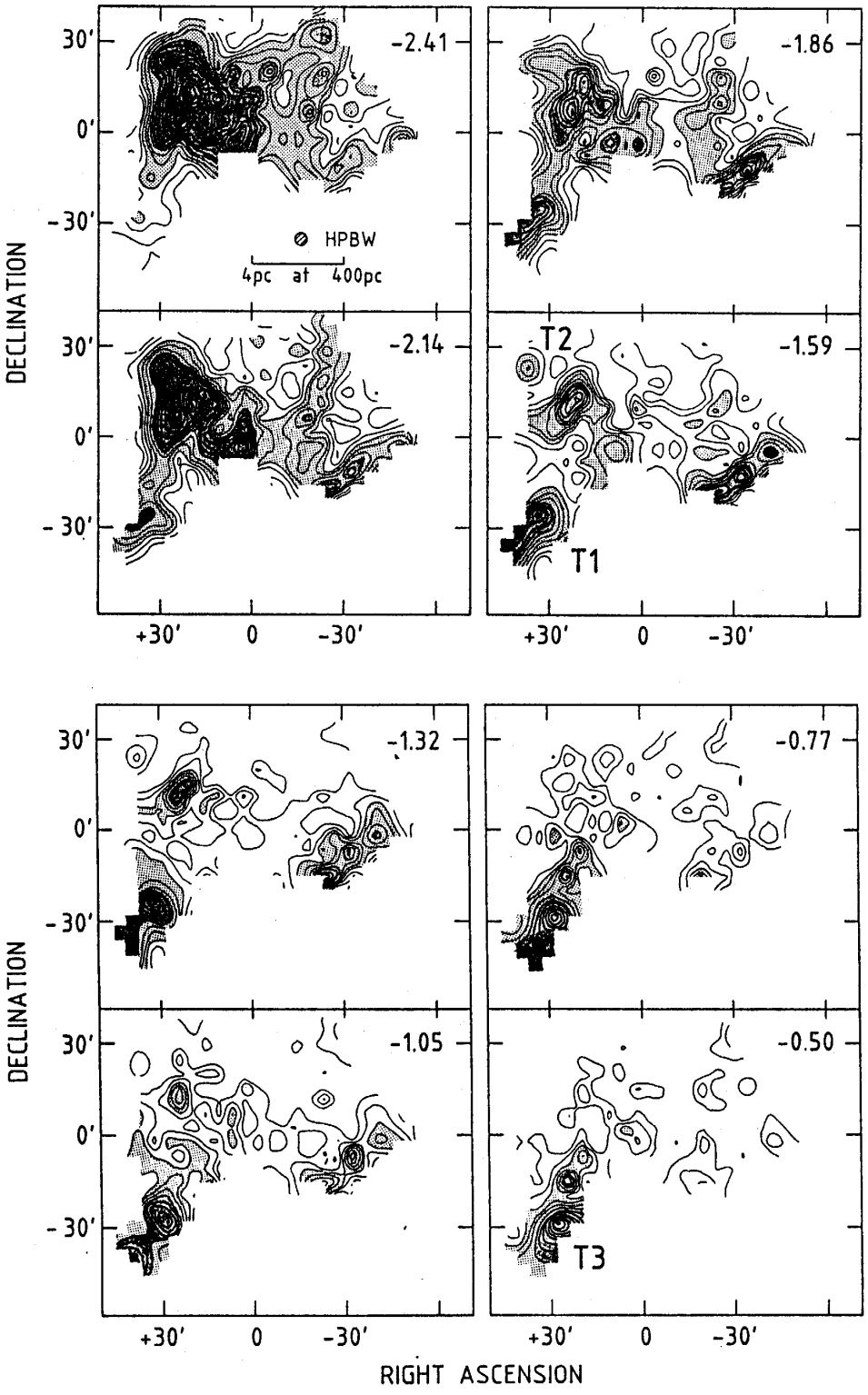

Fig. 4. Channel maps of the Taurus field (reference position $\alpha(1950) = 4h15m01s$, $\delta(1950) = 37°54.6'$) in the $^{13}CO(J=1-0)$ line with 4.4′ resolution. The contour interval is 0.2K. The central velocity of each map is indicated in the upper right corner.

convolution from the beam and the filters, we define a radius $R = 2\sigma_R = 2(\sigma_x^2 + \sigma_y^2)^{1/2}$, a mass of the molecular component $M_{H2} = 6.6 \cdot 10^3 M_\odot A D_{kpc}^2$ (where $A = \int T_A^*(l,b,v)\, dl db dv$ is expressed in K km/s square degrees) and a virial mass $M_v = 1.158\, 10^3 M_\odot \sigma_v^2 R_{pc}$.

Table 1 gives the mean and median values of the cloud parameters which could be defined and easily measured in each complex. It clearly shows that different scales exist in all the complexes which have been studied with large enough a dynamic, but more interesting is the fact, already mentioned in PFP, that the same prominent scales appear with the same characteristics in different complexes, at different distances: this strongly pleads for a real effect and not an observational bias. The most prominent scale (see PFP for the derivation of its parameters) is that of the $1 - 3$ pc clouds already mentioned which appear as the building blocks of the hierarchy: they correspond to the largest scale in which the mass is *distributed* throughout the cloud volume and not concentrated in the units of the subsequent scale. The mean density of these clouds is found to be low: a few $100\,\mathrm{cm}^{-3}$ and their mass is therefore a few $100\,M_\odot$. In what follows, we call *clouds* the elements of this specific scale which are found with similar properties in a variety of environments (see references in FP). They form the first scale in which the local gas density is everywhere close to the mean cloud density.

These *clouds* are often found clustered into larger entities of masses up to several $10^4\,M_\odot$. Although these clusters have always been considered as clouds in the literature, we put some emphasis on the facts that (i) their mass is not as well distributed within their volume as it is in the *clouds* and (ii) their shape is often more elongated or filamentary than that of the *clouds*: we call them *cloud clusters*.

Table 1.

Complex	Distance (kpc)	No. of clouds	$\bar{R}$ (in pc)	R_m (in pc)	$\bar{\sigma}_v$ (in kms^{-1})	$\sigma_{v,m}$ (in kms^{-1})	$\bar{M}$ (in $M_\odot$)	M_m (in $M_\odot$)
TMC1	0.135	1	1.6		0.74		820	
G28+2	0.2	4	0.53	0.51	0.49	0.50	41.5	22.5
G27+4	0.2	3	0.71	0.55	0.58	0.60	60.5	36.7
3C123	0.2	4	0.78	0.73	0.4	0.34	38.5	40
L126	0.5	3	2.6	2.7	1.27	1.08	955	$1.8 \cdot 10^3$
G93+4	0.75	29	1.45	1.35	0.51	0.54	311	180
		5	4.5	4.5	0.85	0.85	$1.5 \cdot 10^3$	$1.5 \cdot 10^3$
		1	60		5.46		$2.3 \cdot 10^5$	
G37+2	2.0	7	4.4	5.5	0.74	0.81	$3.8 \cdot 10^3$	$2.9 \cdot 10^3$
		1	16.7		1.88		$5.6 \cdot 10^4$	
L111P	3.2	6	14	15	1.37	1.5	$5.2 \cdot 10^4$	$3.7 \cdot 10^4$
L111M	3.2	5	7.4	6.9	0.95	1.04	$1.1 \cdot 10^4$	$1.2 \cdot 10^4$

We were able, in two cases, to compare the total molecular mass of such massive *cloud clusters* with the sum of the masses of the constituent *clouds* (i.e. isolated as *clouds* in the $T_A^*(l,b,v)$ distribution of the *cloud clusters* following the procedure described

above): in both cases we find that 50% of the *cluster* mass lies in the *clouds*. The first one is a $2.6 \cdot 10^3 M_\odot$ cluster in G94+3 within which 7 *clouds* have been isolated :

$$\sum_{n=1}^{7} M_{cloud\ n}/M_{cluster} = 0.49.$$

The second is the 32 km/s cluster in G37+2 which is also decomposed into 7 subunits, more massive than the *clouds* defined above. In that case we find that

$$\sum_{n=1}^{7} M_{subunit\ n}/M_{cluster} = 0.48.$$

Another conspicuous scale is that of the $0.1 - 0.2$ pc cores which are found, with similar mass, size and internal velocity dispersion (close to the sound speed in molecular hydrogen), within *clouds* even as diffuse as C2. In any case, they always contain a low fraction ($\sim 10\%$) of their parent *cloud* mass.

Figs. 5a-c display the clouds (*clouds*, *clusters* and *complexes*) parameters derived from the ^{13}CO large scale observations in the form of plots of molecular mass versus radius, internal velocity dispersion versus radius and virial mass versus molecular mass. In all three figures there is an increasing scatter of the data points towards small scales close to the angular and frequency resolution. However, the flattening of the data point ensemble in the $\sigma_v(R)$ relation may be real: σ_v is indeed the velocity dispersion derived from the total linewidth which results from a convolution of non-thermal and thermal motions.

No attempt was made to fit single power laws across the present data points and compare them with those found by other authors on different samples (Larson 1981, Dame et al. 1986) for several reasons of increasing importance: (i) the molecular lines used for the observations are not the same, (ii) the techniques used to define the clouds and their parameters differ from one author to the other and (iii) according to the results of PFP, the hierarchy observed from 0.1 pc to 100 pc is *not self-similar*: if, in the largest scales, the mass of the molecular gas is concentrated in the clouds of the subsequent scales which occupy only a tiny fraction of the total scale volume, this is less and less true going down toward the small scales. It means that the different scales are not governed by the same physics, namely: the respective roles of the thermal energy and magnetic (or turbulent) internal energy in balancing gravity are clearly different at the different scales (see Falgarone and Puget 1986, FP2). In addition, the ambient pressure increases towards small scales and therefore plays an increasing role in the virial balance of the low-mass clouds(Keto and Myers 1986).

The numerical relations given in FP2 have been eyes-fitted through a set of data points which includes our own derivations of the mass, velocity dispersion and size of nine GMC's identified in early ^{12}CO data of Dame (private communication).

Fig. 5c shows that all the scales are approximately (within a factor of 3) in virial balance between gravity and their total kinetic energy (thermal plus nonthermal). The eyes-fit relations given in FP2 are drawn on Figs. 5a and 5b. They suggest

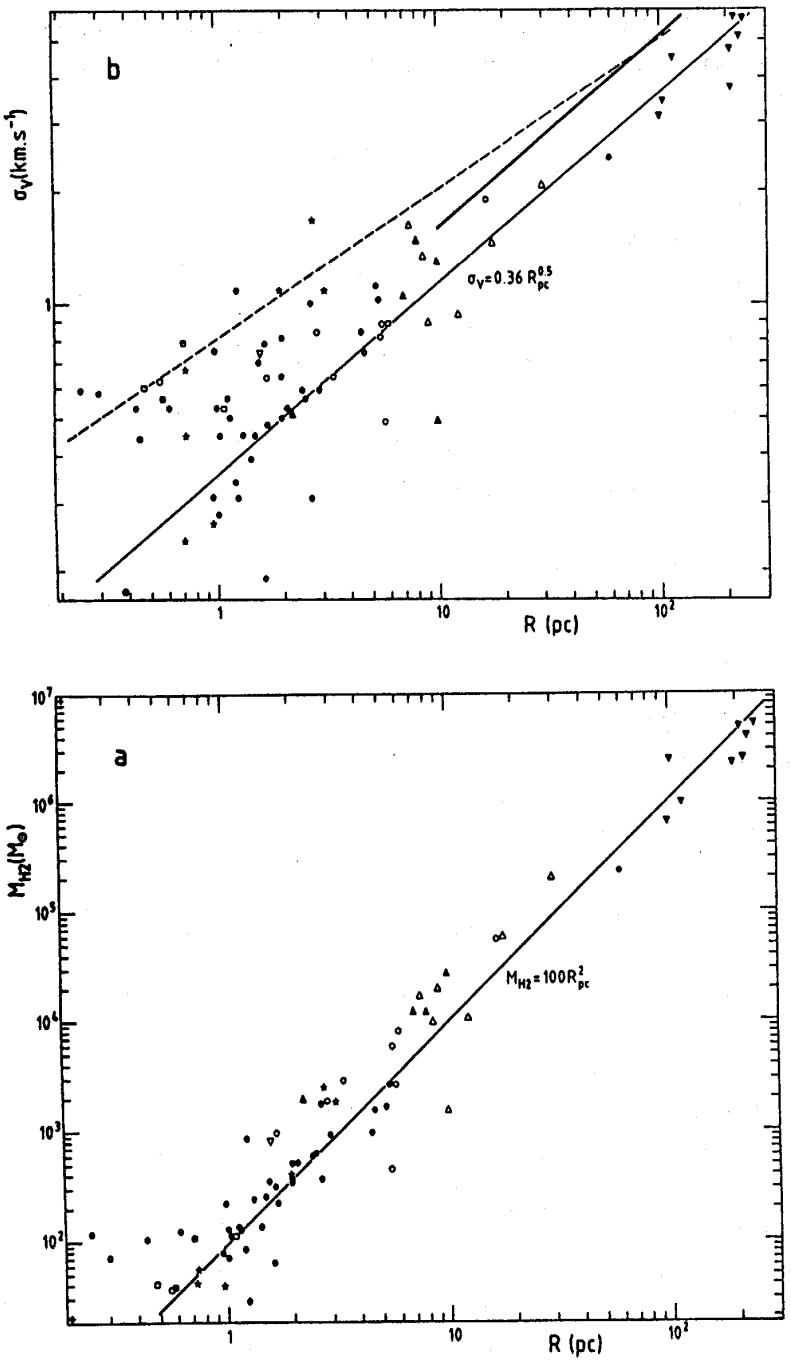

Fig. 5a,b. (a) Plot of molecular mass (derived as explained in the text from the ^{13}CO(J=1-0) line data) versus radius of *clouds* in a variety of *complexes*: G27+4 and G28+2 (open and solid squares respectively), TMC1 (open triangle pointing down), G37+2 (open circles), G111A and G111B (open and solid triangles pointing up respectively), G94+3 (solid circles), G126 (open stars), 3C123 (solid stars) and the values derived from Dame's data (solid triangles pointing down). The solid line is the mass vs. size relation given in FP2. (b) Plot of total internal velocity dispersion versus radius for the same set of *clouds*. The solid line is the σ_v vs. R relation of FP2, the heavy line represents the same relation derived by Dame et al. (1986) from their GMC's set, expressed in term of σ_v and the dotted line is the Larson's (1981) relation.

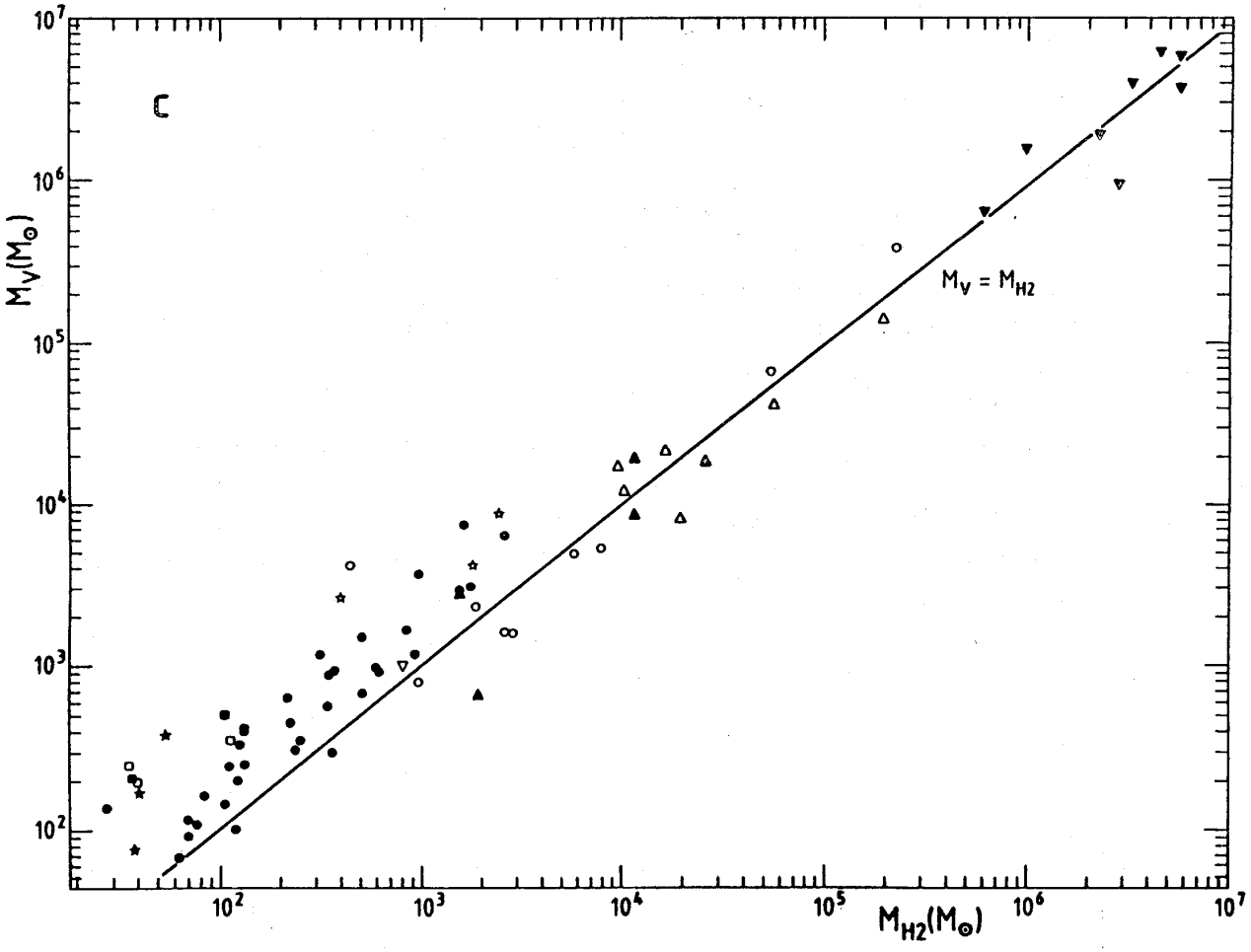

Fig. 5c. Plot of virial mass versus molecular mass for the same set of *clouds*. The solid line traces $M_{H2} = M_v$.

that for all the scales larger than that of the clouds (say above ~ a few pc), including the molecular complexes studied by Dame et al. (1986),

$$M_g \propto R^2 \quad , \quad \sigma_v^{nt} \propto R^{1/2} \quad , \quad M_g \sim M_{vir}.$$

(where σ_v^{nt} is the contribution of non-thermal motions to the internal velocity). These relations imply that the mean density follows

$$\bar{n} \propto R^{-1}$$

for the observed scales (up to a few 100 pc) in which gravity is balanced by non-thermal motions.

2. Magnetic support of the supersonic internal velocity field of clouds

According to a few optimists, the question of the long term support of the supersonic internal velocity field of molecular clouds stops to be critical once these clouds have started to form stars: the total amount of mechanical energy contained in molecular flows driven by stellar winds or in ionization fronts is apparently large enough to balance the dissipation rate of supersonic motions. The problem which remains, however, is the redistribution of this energy to the whole volume of the parent cloud. One step was made, years ago, by Arons and Max (1975) who proposed that Alfvén waves generated by the expansion of HII regions could transfer the energy and momentum of ionization fronts to the surrounding medium.

A different question is: what is the long term support for the supersonic velocity field inside clouds before they start forming stars? Falgarone and Puget (1986, FP2) have proposed a mechanism to support the supersonic random motions within *clouds*, as defined in Section 1, over timescales of the order of several 10^7 yrs. In this mechanism, the hydromagnetic (HM) waves are generated by the entanglements of the field lines moving with the clouds to which they are attached (Clifford and Elmegreen 1983). It is interesting to note that this mechanism also holds for HI clouds, as long as they are not isolated but belong to a complex with neighbours at a mean distance not much larger than their own size.

However, contrary to what is suggested by Myers (1987), the mere fact that a cloud be crossed by Alfvén waves is not a sufficient condition to explain its supersonic (but subalfvénic) observed linewidths : even though the feeding rate is comparable to the dissipation rate of the waves, an internal velocity dispersion of amplitude comparable to the Alfvén velocity can only be generated if the wavelengths are comparable or smaller than the cloud size and if the amplitude of the perturbation of the magnetic field is of the order of the field itself. Unfortunately, in the case of magnetic collisions between clouds, the wavelengths of the perturbations are large: of the order of the collisional mean free path of the clouds within the complex. Such long waves cannot reproduce the amplitude of the observed velocity dispersion. Indeed, these waves do generate a significant velocity dispersion inside the clouds because they are partially reflected by the sharp edges of the clouds and thus create a system of *trapped* waves in which the higher harmonic terms (of smaller wavelengths) are present and contain the required energy. We simply recall here the main results reported and discussed in FP2.

2.1. Gas field coupling

A fundamental and interesting property of a molecular *complex* of the kind described in Section 1, is the following: the intercloud gas is not coupled to the magnetic field for all perturbations of periods shorter than 10^8 yrs and the Alfvén velocity there is so large that the field lines between the clouds may be considered as straight in this range of periods. At the opposite, the gas within the clouds is tightly coupled to the

magnetic field for all perturbations of periods longer than $\sim 10^4$ yrs. These limits only depend upon the density and ionization degree of each medium.

We have computed the stationary field value reached when the field lines drift freely through a self-gravitating cylindrical cloud aligned along the field. In this computation, we have used the density and ionization structure computed in FP which leads to the relation $xn \propto n^{0.4}$ between the ionization degree and the density. The result is a magnetic field value of $B = 10 - 30\,\mu$G quasi-uniform throughout the bulk of the cloud volume and reached, whatever the initial conditions, after a few 10^7 yrs. This crude estimate is in good agreement with the values of $B_{\|}$ measured by Troland and Heiles (1986).

The large density contrast between the clouds and the intercloud medium has therefore three interesting consequences: (i) for the hydromagnetic waves of interest, the gas inside the clouds is well coupled to the magnetic field while the intercloud is not, (ii) the Alfvén velocity is about ten times larger between the clouds than inside despite the increase of the magnetic field across the cloud boundary and (iii) there is a non negligible fraction of the energy of the HM waves which is reflected into the cloud at the cloud boundary.

2.2. The transfer of kinetic energy for one entanglement

During a magnetic entanglement of field lines, the kinetic energy stored in the orbital motions is progressively converted into magnetic energy in the intercloud medium and into kinetic energy within the clouds themselves. When both clouds stop in the center of mass frame, the intercloud magnetic energy and the cloud internal kinetic energy both reach a maximum: the former subsequently decreases and is ultimately converted back into cloud orbital energy and the latter (which is only a small fraction of the total energy) is mostly dissipated. The timescale for the whole cycle is of the order of a few 10^6 yrs for the parameters adopted here. The quantitative results given below have been obtained with an analytical treatment of the equations of motions and $\vec{B}$ behaviour when shear only is considered (Clifford and Elmegreen 1983). The wavelengths and the amplitudes of the Alfvén modes generated within the clouds by such entanglements depend on only two parameters: the cloud Alfvén crossing time, $\tau_A = 2R/v_A$ and the ratio $b/2R$ between the impact parameter of the collision and the cloud size.

As is seen in Fig. 5b of FP2, the resultant velocity dispersion v_{rms} follows closely the amplitude of the second harmonic and its dependence on the parameters of the complex writes:

$$v_{rms} = 0.6\,\mathrm{km/s}\left(\frac{V_{cc}}{3\,\mathrm{km/s}}\right)\left(\frac{b}{2R}\right)^{-1.2}$$

where V_{cc} is the mean orbital cloud velocity in the potential well of the complex and the Alfvén velocity within the clouds has been taken $v_A = 2\,\mathrm{km/s}$. The encouraging point is that, despite the crudeness of the model, the rms velocity generated within a cloud by only one entanglement with one of its neighbours at the most probable distance is of the

order of the observed values. Note also that in all cases the power in discrete modes of the velocity field decreases more steeply than K_n^{-2} (Fig. 7 of FP2) where K_n is the mode wavenumber.

2.3. Internal velocity dispersion resulting from multiple interactions

A more realistic prediction of the internal velocity dispersion takes into account the steepening of the waves which, after randomization, have transferred 2/3 of their energy into the magnetosonic modes, 1/3 only remaining in the shear modes (Zweibel and Josafatsson 1983). The internal velocity field at a given time therefore results from the waves excited by previous entanglements and not yet dissipated, added quadratically to those excited by the current one. The resulting rms velocity:

$$V_{rms} = 0.46\,\mathrm{km/s}\left(\frac{V_{cc}}{3\,\mathrm{km/s}}\right)^{1/2}\left(\frac{v_A}{2\,\mathrm{km/s}}\right)^{1/2}\left(\frac{N_c}{3\cdot 10^{-3}\,\mathrm{pc}^{-3}}\right)^{1/4}\left(\frac{R}{1.5\,\mathrm{pc}}\right)^{-1/4}$$

only weakly depends on all parameters (N_c is the *cloud* number density within the *complex*). It remains proportional to the internal Alfvén velocity if we assume that the field is frozen to the gas during a slow perturbation of the cloud radius:

$$V_{rms} = \gamma v_A$$

with $\gamma = 0.25$ in our model ($v_A \propto R^{-1/2}$). We thus conclude that the average random velocity ($\overline{V}_{int} \sim 2.35\,V_{rms}$) induced within clouds by magnetic interactions with their neighbours follows their internal Alfvén velocity and accounts for their observed linewidths.

2.4. Consequences

This mechanism has two major consequences for the physics of molecular *clouds* (i.e. the 'building blocks' of the *complexes*): (i) unlike isothermal structures, clouds which are supported against gravity by a random velocity field generated as described above, have their internal energy which increases as fast as their gravitational energy during a slow change of their radius:

$$E_{int} \propto V_{rms}^2 \propto R^{-1}$$

This mechanism therefore stabilizes the *clouds* against gravitational collapse. (ii) the steepness of the power spectrum of the internal velocity field may explain the formation of low mass stars within gravitationally stable clouds.

This last point is discussed in Bonazzola et al. (1986). They have shown in 2D simulations of compressible turbulence that a supersonic random velocity field does generate a turbulent pressure. The gradients of that turbulent pressure are found to be correlated with the density gradients which allows the gas to resist gravitational collapse. In this mechanism, large scales are preferentially supported because they contain a larger turbulent energy density.

REFERENCES

Arons, J., and Max, C.E. 1975, *Ap. J. Lett.*, **196**, L77.

Bonazzola, S., Falgarone, E., Heywaerts, J., Pérault, M., Puget, J. L. 1987, *Astron. Astrophys.*, **172**, 293

Clifford, P. and Elmegreen, B.G. 1983, *MNRAS*, **202**, 629.

Dame, T. M. and Thaddeus, P. 1985 , *Ap. J.*, **297**, 751.

Dame,T. M., Elmegreen, B.G., Cohen, R., and Thaddeus,P. 1986, *Ap. J.*, **305**, 892.

Falgarone, E., Puget, J.L., Evans, N.J. Federman, S. 1984 , in *Nearby Molecular Clouds*, Regional IAU Conference, ed. G. Serra.

Falgarone, E., Puget, J. L. 1985, (FP) *Astron. Astrophys.*, **142**, 157.

Falgarone, E., Puget, J. L. 1986, (FP2) *Astron. Astrophys.*, **162**, 235.

Gispert, R., Puget, J. L., Serra, G. 1982, *Astron. Astrophys.* **106**, 293.

Keto, E., Myers, P. 1986, *Ap.J.*, **304**, 466.

Larson, R. B. 1981, *MNRAS*, **194**, 809.

Myers, P. C. 1987, in *Summer School on Interstellar Processes*, eds. D. Hollenbach and H. Thronson (Dordrecht, Reidel), in press.

Pérault, M., Falgarone, E., Puget, J. L. (PFP) 1985, *Astron. Astrophys.*, **152**, 371.

Pérault, M., Falgarone, E., Puget, J. L. 1986, *Astron. Astrophys.*, **157**, 139.

Pérault, M., Falgarone, E. 1987 in preparation.

Troland, T. H., Heiles, C. 1986, *Ap. J.*, **301**, 339.

Ungerer, V., Mauron, N., Brillet, J., Nguyen Quang Rieu 1985, *Astron. Astrophys.*, **146**, 123.

Zweibel, E. G., Josafatsson, K. 1983, *Ap. J.*, **270**,511.